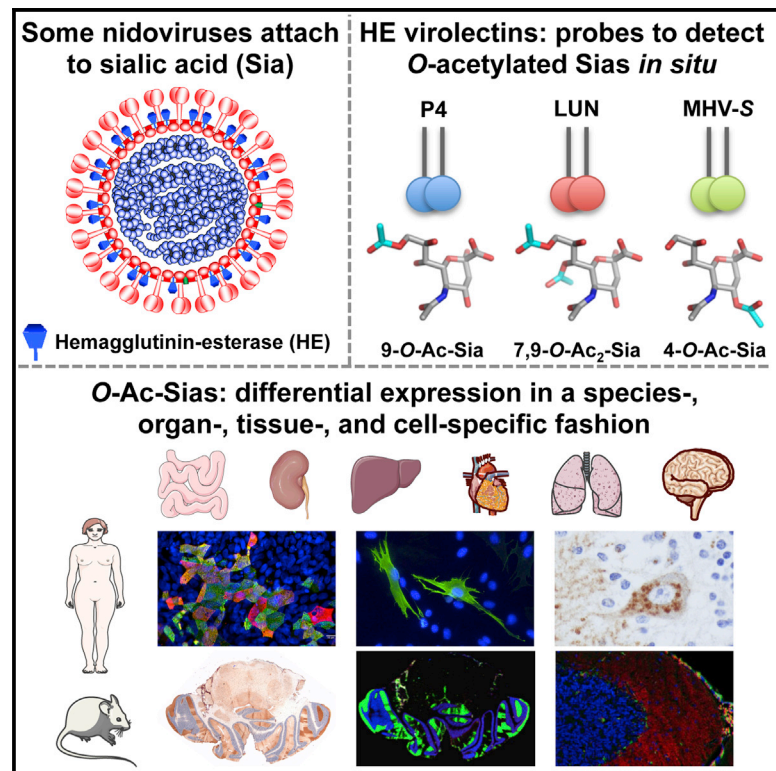# Cell Reports

# Complexity and Diversity of the Mammalian Sialome Revealed by Nidovirus Virolectins

## Graphical Abstract



## Authors

Martijn A. Langereis, Mark J.G. Bakkers, Lingquan Deng, ..., Ajit Varki, Johannis P. Kamerling, Raoul J. de Groot

## Correspondence

r.j.degroot@uu.nl

## In Brief

Postsynthetically modified sialic acids serve as critical tags in biomolecular recognition events, both in health and disease. Langereis et al. introduce methodology, based on nidovirus lectins and enzymes, for in situ detection of distinct *O*-acetylated sialic acid species and demonstrate its applicability by exploring sialoglycan distribution in mammalian cells and tissues.

## Highlights

- Virolectins detect and distinguish between closely related *O*-Ac-Sias in situ

- *O*-Ac-sialoglycans occur in nature in a diversity not appreciated so far

- *O*-Ac-Sias are differentially expressed in a species-, tissue-, and cell-specific fashion

- There is extensive cell-to-cell variability in *O*-Ac-Sia expression in vivo and in vitro

CrossMark

CellPress

# Complexity and Diversity of the Mammalian Sialome Revealed by Nidovirus Virolectins

Martijn A. Langereis,[1,8] Mark J.G. Bakkers,[1,8] Lingquan Deng,[2,9] Vered Padler-Karavani,[2,10] Stephin J. Vervoort,[1] Ruben J.G. Hulswit,[1] Arno L.W. van Vliet,[1] Gerrit J. Gerwig,[3] Stefanie A.H. de Poot,[1] Willemijn Boot,[1] Anne Marie van Ederen,[4] Balthasar A. Heesters,[1,11] Chris M. van der Loos,[5] Frank J.M. van Kuppeveld,[1] Hai Yu,[6] Eric G. Huizinga,[7] Xi Chen,[6] Ajit Varki,[2] Johannis P. Kamerling,[3] and Raoul J. de Groot[1,*]

[1]Virology Division, Department of Infectious Diseases and Immunology, Faculty of Veterinary Medicine, Utrecht University, 3584 CL Utrecht, the Netherlands
[2]Glycobiology Research and Training Center, Departments of Medicine and Cellular and Molecular Medicine, University of California, San Diego, La Jolla, CA 92093-0687, USA
[3]Bio-Organic Chemistry, Bijvoet Center for Biomolecular Research, Faculty of Sciences, Utrecht University, 3584 CH Utrecht, the Netherlands
[4]Department of Pathobiology, Faculty of Veterinary Medicine, Utrecht University, 3584 CL Utrecht, the Netherlands
[5]Department of Cardiovascular Pathology, Free University Amsterdam, 1105 AZ Amsterdam, the Netherlands
[6]Department of Chemistry, University of California, Davis, Davis, CA 95616, USA
[7]Crystal and Structural Chemistry, Bijvoet Center for Biomolecular Research, Faculty of Sciences, Utrecht University, 3584 CH Utrecht, the Netherlands
[8]Co-first author
[9]Present address: Department of Pathology, School of Medicine, Johns Hopkins University, Baltimore, MD 21231, USA
[10]Present address: Laboratory of Glycoimmunology, Department of Cell Research and Immunology, The George S. Wise Faculty of Life Science, Center for Nanoscience and Nanotechnology, Tel Aviv University, Tel Aviv 69978, Israel
[11]Present address: Department of Microbiology and Immunobiology, Harvard Medical School, Boston, MA 02115, USA
*Correspondence: r.j.degroot@uu.nl
http://dx.doi.org/10.1016/j.celrep.2015.05.044

## SUMMARY

Sialic acids (Sias), 9-carbon-backbone sugars, are among the most complex and versatile molecules of life. As terminal residues of glycans on proteins and lipids, Sias are key elements of glycotopes of both cellular and microbial lectins and thus act as important molecular tags in cell recognition and signaling events. Their functions in such interactions can be regulated by post-synthetic modifications, the most common of which is differential Sia-*O*-acetylation (*O*-Ac-Sias). The biology of *O*-Ac-Sias remains mostly unexplored, largely because of limitations associated with their specific in situ detection. Here, we show that dual-function hemagglutinin-esterase envelope proteins of nidoviruses distinguish between a variety of closely related *O*-Ac-Sias. By using soluble forms of hemagglutinin-esterases as lectins and sialate-*O*-acetylesterases, we demonstrate differential expression of distinct *O*-Ac-sialoglycan populations in an organ-, tissue- and cell-specific fashion. Our findings indicate that programmed Sia-*O*-acetylation/de-*O*-acetylation may be critical to key aspects of cell development, homeostasis, and/or function.

## INTRODUCTION

Cells are covered by a dense thicket of glycans. Though attached to proteins and lipids, these oligo- and polysaccharides are more than decoration. With a structural complexity vastly exceeding that of proteins and nucleic acids, they act as molecular tags in cell recognition and signaling events. Mammalian glycans form linear and branched chains of variable size and composition yet commonly with sialic acids (Sias) as terminal, surface-exposed residues. In consequence of this topology, Sias are key elements of the glycotopes of many regulatory cellular lectins (Crocker et al., 2007; Schauer, 2009). For the same reason, they have become attachment factors of choice for a range of pathogens including protozoa, fungi, bacteria, and viruses.

Sias occur in a wide variety, their diversity resulting from differences in glycosidic linkage as well as from differential modifications (Deng et al., 2013). In most mammals, humans excluded, the parental Sia *N*-acetylneuraminic acid (Neu5Ac) can be enzymatically converted to *N*-glycolylneuraminic acid (Neu5Gc) (Chou et al., 1998; Irie et al., 1998). Another common modification is Sia-*O*-acetylation substituting the hydroxyl groups at carbon atoms C4, C7, C8, and/or C9 (Kamerling and Gerwig, 2006; Klein and Roussel, 1998) (Figure S1). In lock-and-key interactions, the presence or absence of these *O*-acetyl moieties can block or promote binding of cellular and microbial lectins, and their controlled addition and removal through sialate-*O*-acetylesterases (SOAEs) and sialate-*O*-transferases (SOATs) may

thus act as a molecular switch to control downstream processes and events. This principle is illustrated by the regulation of peripheral B cell tolerance. Repression of antigen receptor signaling through Sia-dependent binding of Siglec 2/CD22 to the B cell receptor is modulated by Sia-9-$O$-acetylation/de-$O$-acetylation (Cariappa et al., 2009), and defects in SOAE expression may be associated with autoimmunity (Pillai, 2013; Surolia et al., 2010). Defective (de-)$O$-acetylation of Sias has also been implicated in cancer to correlate with metastatic potential, escape from apoptosis and drug resistance (Büll et al., 2014; Ghosh et al., 2007; Mukherjee et al., 2008; Parameswaran et al., 2013).

There is limited understanding of how $O$-acetylation of Sias is regulated, and the role of distinct $O$-acetylated ($O$-Ac) Sias in health and disease remains largely unexplored. A major hurdle for advancement of this field is a lack of convenient experimental approaches that would allow detection of, and distinction between, Sia variants in situ. Viruses that use Sias as receptor determinants come with a treasure trove of lectins and sugar-modifying enzymes (Neu et al., 2011). For example, the hemagglutinin-esterase proteins (HEs) of toro-, corona-, and ortho-myxo-viruses are envelope glycoproteins that mediate reversible virion attachment to $O$-Ac-Sias through the concerted action of distinct lectin and receptor-destroying (SOAE) domains (Figure S1A) (de Groot, 2006; Langereis et al., 2009; Langereis et al., 2012; Zeng et al., 2008). Here, we investigated the biochemical and structural properties of toro- and coronavirus HEs with particular focus on their receptor specificity, and their potential use as tools in explorative sialoglycobiology. We demonstrate that the nidovirus "virolectins" have evolved to bind different $O$-Ac-Sia variants selectively and with such affinity as to allow detection of distinct $O$-Ac-sialoglycan populations in mammalian cells and tissues. We show that $O$-Ac-sialoglycans are expressed differentially in a species-, organ-, tissue-, and cell-type-specific fashion and that their expression is regulated even at the level of the individual cell.

## RESULTS AND DISCUSSION

Toroviruses and group A betacoronaviruses (order *Nidovirales*, family *Coronaviridae*; collectively referred to as nidoviruses throughout) are positive-strand RNA viruses of mammals. Their HEs share a common evolutionary origin with the influenza C hemagglutinin-esterase fusion protein (HEF) and were added to the respective virus proteomes relatively recently (de Groot, 2006; Zeng et al., 2008). In the course of evolution, nidovirus HEs with novel SOAE substrate and lectin ligand specificities arose. In one lineage of rodent coronaviruses, HE ligand and substrate specificity shifted toward 4-$O$-Ac-Sias. Most nidovirus HEs, however, resemble influenza C virus HEF in that they bind to 9-$O$-Ac-Sias in a 9-$O$-acetyl-dependent fashion and function as sialate-9-$O$-acetylesterases (de Groot, 2006). Yet, even among this latter group of HEs, subtle but salient differences in SOAE substrate preference are apparent. For instance, porcine torovirus (PToV) HEs preferentially cleave 9-mono-$O$-Ac-Sias, while those of bovine toroviruses (BToVs) display a preference for 7,9-di-$O$-acetylated substrates (Langereis et al., 2009; Smits et al., 2005). Also, the HEs of bovine coronavirus (BCoV) and

influenza C virus, while more promiscuous in SOAE substrate usage, do show a predilection for 7,9-di- or 9-mono-$O$-acetylated substrates, respectively (Figure S2A). All HEs readily cleave $O$-acetyl groups both from 5-$N$-Gc- and 5-$N$-Ac-Sias, with some HEs displaying a modest preference for the latter type (Figure S2B; for a summary of HE SOAE substrate specificities, see Figure S2C).

To investigate whether SOAE substrate preference for 7,9-di- or 9-mono-$O$-Ac-Sias reflects lectin ligand fine specificity, we expressed a comprehensive set of nidovirus HEs as Fc fusion proteins (Table S1) with the esterase inactivated through an active site Ser-to-Ala substitution (HEs with inactive SOAE are referred to as HE$^0$ throughout; enzymatically active HEs are referred to as HE$^+$).

### Nidovirus HEs: Virolectins of Different Receptor Specificity

HE$^0$-Fc virolectins were tested for Sia binding and ligand specificity by hemagglutination assay with rat red blood cells (RBCs) and by solid-phase lectin binding assay (sp-LBA) with bovine submaxillary mucin (BSM), a natural $O$-glycosylated sialoglyco-conjugate exceptionally rich in ($\alpha$2-6)-linked $O$-Ac-Sias (for an extensive analysis of BSM Sia content, pivotal to this study, see the Supplemental Experimental Procedures, Figures S1C and S1D, and Tables S2 and S3).

Hemagglutination was observed for all nidovirus HEs. Pre-treating RBCs with sialidase prevented hemagglutination, indicating that in each case, agglutination was Sia-dependent (data not shown). Selective depletion of 9-mono-$O$-Ac-Sias from the cell surface with PToV HE$^+$ prevented hemagglutination by HE$^0$-Fc of PToV strains Markelo and P4 but left that by BCoV, equine coronavirus (ECoV), and BToV virolectins largely unaffected. Conversely, depletion of 7,9-di-$O$-Ac-Sias with BToV-Breda HE$^+$ prevented hemagglutination by BCoV, ECoV, and BToV HEs but did not reduce agglutination by PToV HE. De-$O$-acetylation with BCoV HE$^+$, which accepts both 9-mono- and 7,9-di-$O$-acetylated substrates (Figure S2), abrogated hemagglutination by all virolectins (Figure 1A).

In solid-phase assays, all HEs, except for 4-$O$-Ac-Sia-specific MHV-$S$ HE$^0$ (Langereis et al., 2012), bound to BSM in a 9-$O$-Ac-Sia-dependent fashion (data not shown), albeit with markedly varied affinities (Figure 1B). Those of ECoV-NC99, BCoV-Mebus and -LUN, and PToV-P4 bound exceptionally well and were therefore studied further.

In accordance with the hemagglutination analyses, binding of ECoV-NC99, BCoV-Mebus, and BCoV-LUN HE$^0$ was lost upon SOAE predigestion of BSM with either BCoV or BToV HE$^+$ but relatively resistant to de-$O$-acetylation of Sias by PToV HE$^+$. Conversely, binding of PToV-P4 HE$^0$ was highly sensitive to pretreatment of BSM with PToV HE$^+$, less sensitive to BCoV HE$^+$, and even far less so to BToV HE$^+$ (Figure 1C).

Apparently, the differences between the ECoV and BCoV HEs on the one hand and PToV-P4 HE on the other arise from a preference or intolerance for di-$O$-acetylation at the Sia glycerol side chain. As a direct test, we performed sp-LBA with BSM, chemoenzymatically converted to carry 9-mono-$O$-Ac-Sias exclusively (Figure 1D). To this end, BSM was first digested with excess BCoV HE$^+$ to selectively remove all Sia-9-$O$-acetyl moieties
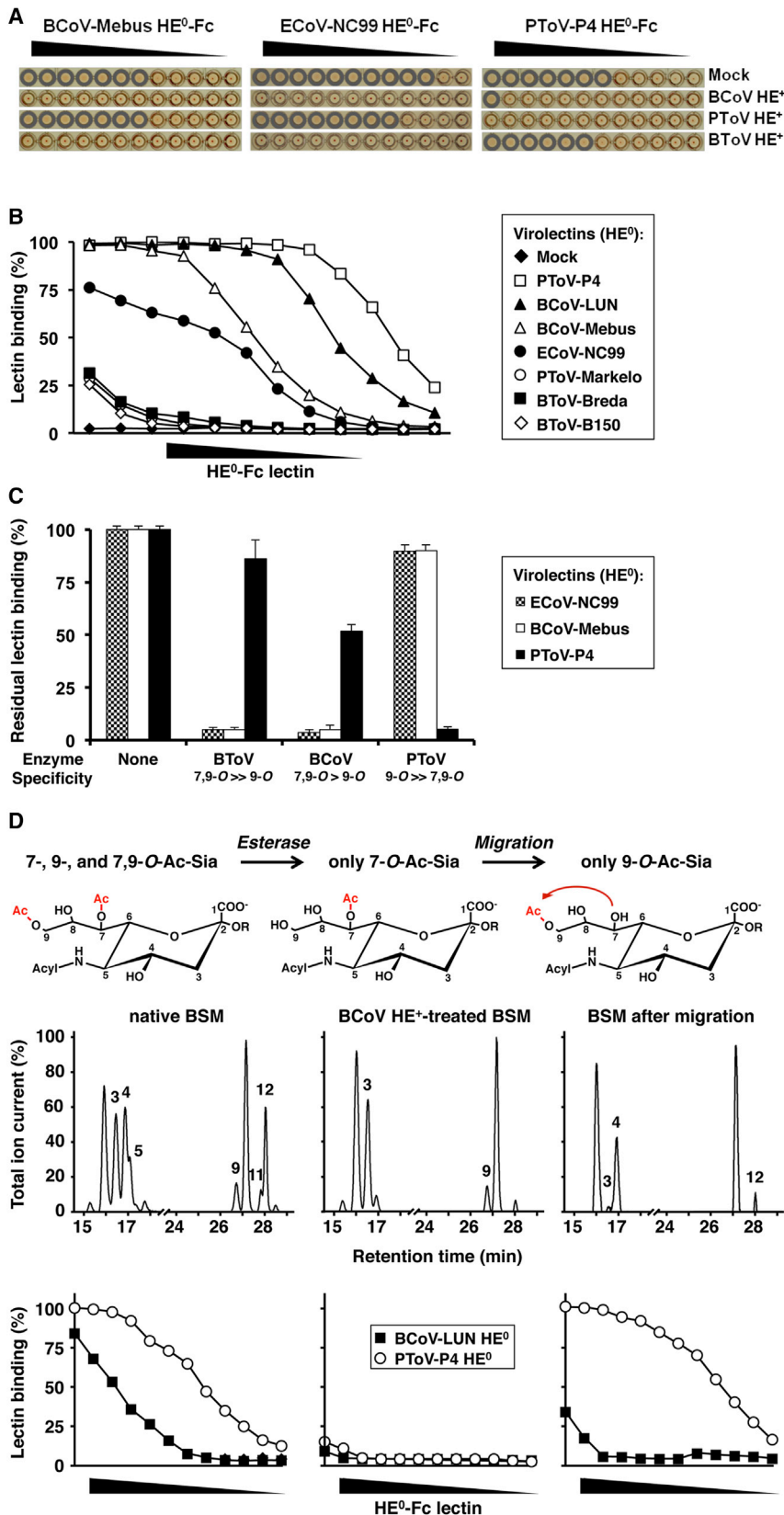
**Figure 1. Nidovirus Virolectins Distinguish between 9-Mono-*O*- and 7,9-Di-*O*-Ac-Sias**

(A) Hemagglutination assay with 2-fold serial dilutions of esterase-inactive $HE^0$-Fc virolectins. Prior to hemagglutination assay, RBCs were mock treated, depleted for *O*-Ac-Sias with BCoV-Mebus $HE^+$-Fc, or selectively depleted for 7,9-di-*O*- or 9-mono-*O*-Ac-Sias with BToV-Breda or PToV-Markelo $HE^+$-Fc, respectively. Wells positive for hemagglutination are encircled.

(B) Nidovirus HEs bind to *O*-Ac-Sias in BSM with widely different affinities. Lectins (in 2-fold serial dilutions, starting at 0.1 μg/μl were compared by sp-LBA for relative binding to BSM (OD450 value for 0.1 μg/μl PToV-P4 $HE^0$-Fc set at 100%). Data presented as mean ± SD. Descending concentrations of $HE^0$-Fc virolectins, plotted on the x axis, are schematically indicated by black descending triangles.

(C) sp-LBA with BSM, after on-the-plate depletion for distinct *O*-Ac-Sia populations with BCoV-Mebus, BToV-Breda, or PToV-P4 $HE^+$-Fc. Receptor destruction was assessed by sp-LBA with BCoV-Mebus or PToV-P4 $HE^0$-Fc at fixed concentrations (5 ng/μl and 1 ng/μl, respectively).

(D) Differences in receptor preference between BCoV-LUN and PToV-P4 HE revealed by chemo-enzymatical modification of BSM *O*-Ac-Sia content. Top: experimental outline. Middle: gas-liquid chromatography-electron ionization mass spectrometry (GLC-EIMS) profiles of corresponding BSM preparations (peaks are numbered as in Table S2: peak 3; β-Neu5,7Ac₂, peak 4; β-Neu5,9Ac₂, peak 5; β-Neu5,7,9Ac₃, peak 9; β-Neu5Gc7Ac, peak 11; β-Neu5Gc7,9Ac₂, peak 12; β-Neu5Gc9Ac). Bottom: sp-LBA as in (B).
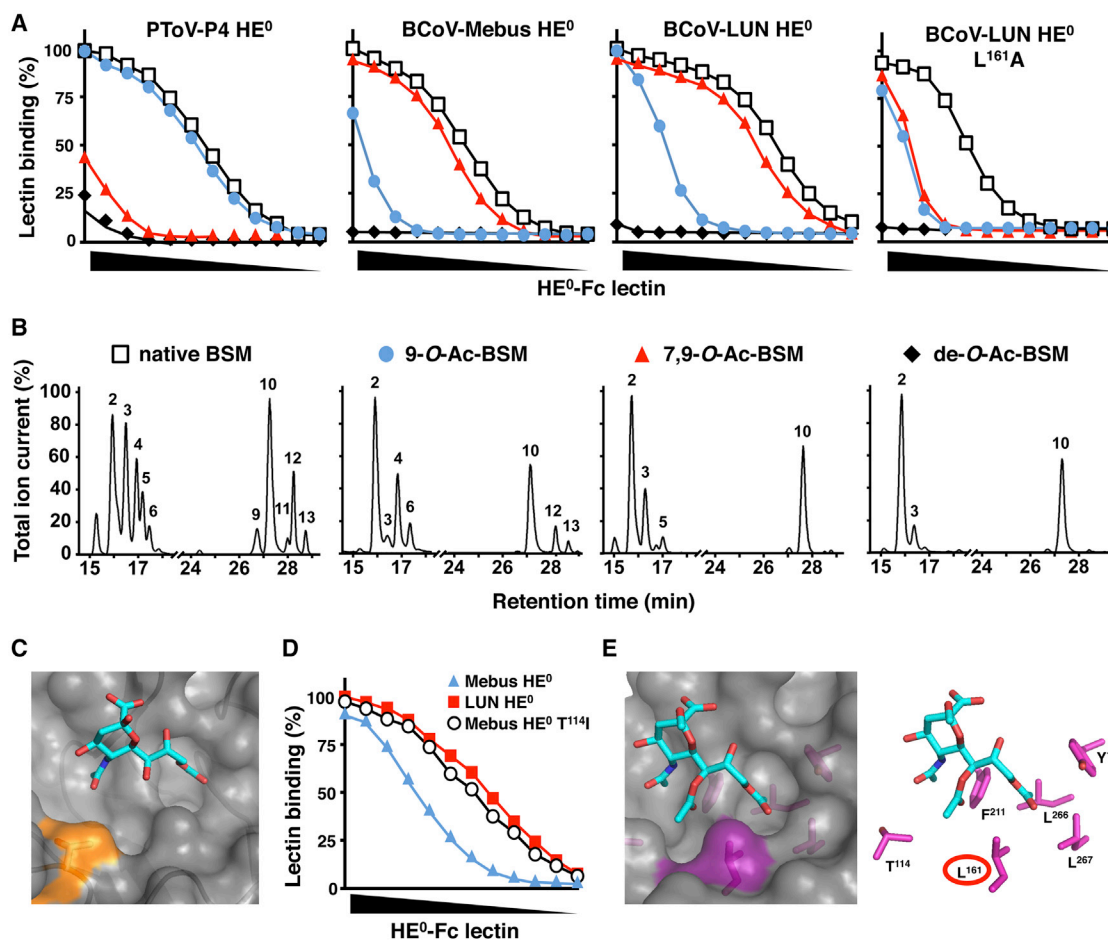
See also Figure S1 and Table S1.

**Figure 2. Nidovirus Virolectins Display Distinct *O*-Ac-Sia Specificity**

(A) sp-LBA as in (Figure 1B) with native and mutant virolectins (HE[0]-Fc of PToV-P4, BCoV-Mebus, and BCoV-LUN and BCoV-LUN/L[161]A) and BSM preparations of defined Sia content. Non-modified BSM (native); BSM, mono-specific for 9-mono-*O*-Ac-Sias (9-*O*-Ac-BSM), or 7,9-di-*O*-Ac-Sias (7,9-*O*-Ac-BSM); BSM, depleted for all *O*-Ac-Sias (de-*O*-Ac-BSM). Relative binding (in percentages) was calculated with binding to native BSM set at 100%. BSM preparations were calibrated by dilution in coating buffer such as to ensure that the amounts of remaining *O*-Ac-Sia species in 9-*O*-Ac- and 7,9-di-*O*-Ac-BSM preparations were comparable to those in native BSM.

(B) GLC-EIMS profiles of corresponding BSM preparations (peaks numbered as in Table S2: peak 2; β-Neu5Ac, peak 3; β-Neu5,7Ac$_2$, peak 4; β-Neu5,9Ac$_2$, peak 5; β-Neu5,7,9Ac$_3$, peak 6; α-Neu5,9Ac$_2$, peak 9; β-Neu5Gc7Ac, peak 11; β-Neu5Gc7,9Ac$_2$, peak 12; β-Neu5Gc9Ac, peak 13; α-Neu5Gc9Ac).

(C) Surface representation of the receptor binding site of BCoV-Mebus HE in complex with α-Neu5,9Ac$_2$2Me (PDB: 3CL5); the patch, contributed by T[114], is colored in orange.

(D) Difference in affinity between BCoV-Mebus and -LUN HE[0] attributed to a single amino acid change in the Sia binding site. Virolectins were compared for relative binding to BSM by sp-LBA as in (Figure 1B).

(E) Surface and stick representations of the BCoV-Mebus HE lectin site in complex with α-Neu5,7,9Ac$_3$2Me as modeled by molecular docking (Trott and Olson, 2010). L[161] is highlighted. Note the proximity of the L[161] side-chain to the Sia-7-*O*-Ac-methyl (~3.8 Å), favorable for van der Waals interaction, and the burying of hydrophobic surface.

while leaving 7-*O*-acetyl groups attached. In result, binding of both BCoV-LUN and PToV-P4 HE[0] was lost (Figure 1D), formally demonstrating that Sia-9-*O*-acetylation is a strict requirement and that 7-mono-*O*-Ac-Sias do not serve as ligands. Upon pH/temperature-induced C7-to-C9 migration of *O*-acetyl moieties (Kamerling et al., 1987) as to produce 9-mono-*O*-Ac-Sias, binding of PToV-P4 HE[0] was restored to levels even beyond those in native BSM (note that in native BSM, the amount of 7-*O*-Ac- and 7,9-di-*O*-Ac-Sias combined is almost twice that of 9-mono-*O*-Ac-Sias; Tables S2 and S3). Binding of BCoV-LUN HE[0], how-

ever, was restored only partially (Figure 1D). The results show that PToV-P4 HE[0] is a high-specificity lectin for 9-mono-*O*-Ac-Sia. Conversely, BCoV-Mebus and BCoV-LUN HE[0] accept 9-mono-*O*-Ac-Sias but bind to 7,9-di-*O*-Ac-Sias with much higher affinity (Figures 2A and 2B).

Although the BCoV and ECoV HEs would seem to favor 7,9-di-*O*-Ac-Sias, their binding characteristics in sp-LBA indicate a difference in ligand preference. The ECoV-NC99 binding curve is suggestive of high-affinity binding to select glycotopes that are present in BSM in amounts considerably lower than those of

BCoV HE (Figure 1B). Thus, ECoV HE may preferentially bind to a subpopulation of the BCoV HE ligands or bind a distinct 9-*O*-Ac-Sia variant altogether. The combined results establish that the ECoV-NC99, BCoV-Mebus/LUN and PToV-P4 virolectins each have distinct ligand preferences and distinguish between closely related 9-*O*-Ac-Sia populations.

### Structural Evidence that BCoV HE Preferably Binds 7,9-Di-*O*-Ac-Sias

The structure of BCoV-Mebus HE, complexed with a synthetic 9-*O*-Ac-Sia analog, was solved to 1.8 Å (Zeng et al., 2008). BCoV-LUN HE differs from that of BCoV-Mebus in only seven residues, one of which is in a loop at the rim of the Sia binding site (Figure 2C). This single amino acid variation (T$^{114}$ in BCoV-Mebus, I$^{114}$ in BCoV-LUN HE) fully accounts for the observed 3-fold difference in binding affinity toward BSM (Figures 1B and 2D). Apparently, the Thr/Ile substitution does not alter lectin ligand preference for 7,9-di-*O*- over 9-mono-*O*-Ac-Sias; as compared to BCoV-Mebus HE, LUN HE displays equally increased affinities for either Sia type (Figure 2A). Based on the position of T$^{114}$ relative to the bound ligand, its exchange by Ile may affect, directly or indirectly, binding site interactions with the Sia-5-*N*-acyl moiety. Although not immediately obvious from replacement modeling how this would be achieved, such interactions may raise binding affinity for Sia per se but, as indicated by glycan array analysis (*vide infra*), also alter the lectin's relative preference for 5-*N*-Ac- or 5-*N*-Gc-Sias.

To determine the structural basis for BCoV HE's ligand preference for di-*O*-Ac-Sias over 9-mono-*O*-Ac-Sias, we examined the lectin-Sia interface with particular focus on protein-sugar interactions at the Sia glycerol side chain. The Sia 9-*O*-Ac group, crucial to receptor binding, docks into a hydrophobic pocket. The vicinity of Sia glycerol atom C8 is crowded such that substitution of an *O*-Ac moiety for the C8 hydroxyl is not possible without introducing steric strain. Hence, the structure of the BCoV HE receptor binding site appears incompatible with binding of 8-*O*-Ac-Sias. There is, however, ample space to accommodate modifications at C7. Moreover, modeling of Neu5,7,9Ac$_3$ in the lectin binding site revealed potential interactions between the Sia-7-*O*-Ac moiety and the side chains of F$^{211}$ and L$^{161}$ that could contribute to the lectin's preference for 7,9-di-*O*-Ac-Sias (Figure 2E). Accordingly, L$^{161}$A substitution strongly decreased binding to BSM, yet, as demonstrated for BCoV-LUN HE, high-affinity binding to 7,9-di-*O*-Ac-Sias was affected more than low-affinity binding to 9-mono-*O*-Ac-Sias (Figure 2A). In effect, ligand fine specificity was lost, the substitution causing the BCoV-LUN HE L$^{161}$A mutant to now bind each receptor type equally poorly.

### Glycan Microarray Analysis of Nidovirus Virolectins

Conceivably, HE ligand preference could be influenced by (1) the presence or absence of other Sia modifications such as 5-*N*-glycolylation, (2) the type of glycosidic linkage, and/or (3) the overall composition and structure of the underlying glycan (Deng et al., 2013). We therefore systematically compared the binding properties of the HEs of BCoV-LUN, BCoV-Mebus, ECoV-NC99, and PToV-P4 toward paired (Neu5Ac- or Neu5Gc-based, and α2-3 or α2-6-linked) 9-*O*-Ac and non-*O*-Ac-sialoglycans by glycan mi-

croarray analysis (Padler-Karavani et al., 2011; Padler-Karavani et al., 2012). The results, summarized in Figures 3A and S3, indicate that all four lectins accept both α2-3- and α2-6-linked 9-*O*-Ac-Sias, though with noted exceptions apparently related to overall glycan structure/composition. The most prominent and consistent difference was in the relative binding preference for Sias, differentially modified at C5. The PToV-P4 and ECoV-NC99 lectins displayed a clear binding bias and strongly favored 5-*N*-Ac-Sias. Conversely, BCoV-LUN and Mebus HEs more readily accepted both 5-*N*-Ac- and 5-*N*-Gc-Sias, albeit depending on the underlying glycan structure. Of the two lectins, BCoV-LUN HE bound more strongly to all ligands, in accordance with sp-LBA data (Figure 1B), and displayed a higher apparent affinity for 5-*N*-Gc-Sias. The results provide a clue to the observed difference between BCoV and ECoV-NC99 HEs in sp-LBA (Figure 1B). BSM predominantly carries sialyl-Tn-type *O*-glycans (Kozak et al., 2012), represented in the microarray by glycans #23 and #24. In contrast to the BCoV HEs, ECoV-NC99 HE binds 9-*O*-Ac-5-*N*-Ac-sialyl Tn exclusively (glycan #23; Figure 3A) and not to its 5-*N*-glycolylated variant (glycan #24) and hence would recognize only a subpopulation of the BCoV HE glycotopes.

Although glycan array analysis provides insight into the binding properties of the lectins, caution is warranted, as the number of glycans included in the array is limited and does not reflect the full spectrum of natural *O*-Ac-sialoglycans. Sias with multiple *O*-Ac moieties are absent, as are multi-antennary sialoglycans. Furthermore, differences in binding as detected by glycan array analysis may occur from differences in presentation and/or flexibility of the printed glycans and from how such variables would affect multivalent lectin-Sia interactions (Padler-Karavani et al., 2012). Finally, the biophysical and biological consequences of modest differences in binding preference as detected by glycan array analysis are difficult to predict. Such differences may be augmented and of major significance during multivalent HE-mediated virion attachment in vivo. Conversely, viral attachment to suboptimal ligands may well occur, if such glycans are present in high local densities. At any rate, the 9-*O*-Ac-sialoglycan populations recognized by the PToV, BCoV, and ECoV virolectins cannot be defined in absolute terms. Their binding profiles, while unique, partially overlap. PToV-P4 would seem to be the most specific in that it displays a strong predilection for 9-mono-*O*-acetylated, 5-*N*-acetylated Sias, and BCoV-LUN HE the least (for a summary of binding profiles, see Figure 3B).

### Differential Expression of 4-*O*- and 9-*O*-Ac-Sias in Cultured Mammalian Cells

Various reagents have been used to detect *O*-Ac-Sia species, including lectins of the African landsnail *Achatina fulica* (Ghosh et al., 2007; Mukherjee et al., 2008) and Californian crab *Cancer antennarius* (Parameswaran et al., 2013), salmon infectious anemia virus HE extracted from infected cells (Aamelfot et al., 2014), and the heterologously expressed ectodomain of influenza C HEF (Cariappa et al., 2009; Klein et al., 1994; Krishna and Varki, 1997; Shi et al., 1996, 1998; Sjoberg et al., 1994). The present study extends previous work in that it builds on a comprehensive set of viral lectins and SOAEs, extensively characterized both in terms of structure and ligand/substrate fine specificity. In combination with *MHV-S* HE$^0$, the virolectins of PToV-P4, ECoV-NC99,
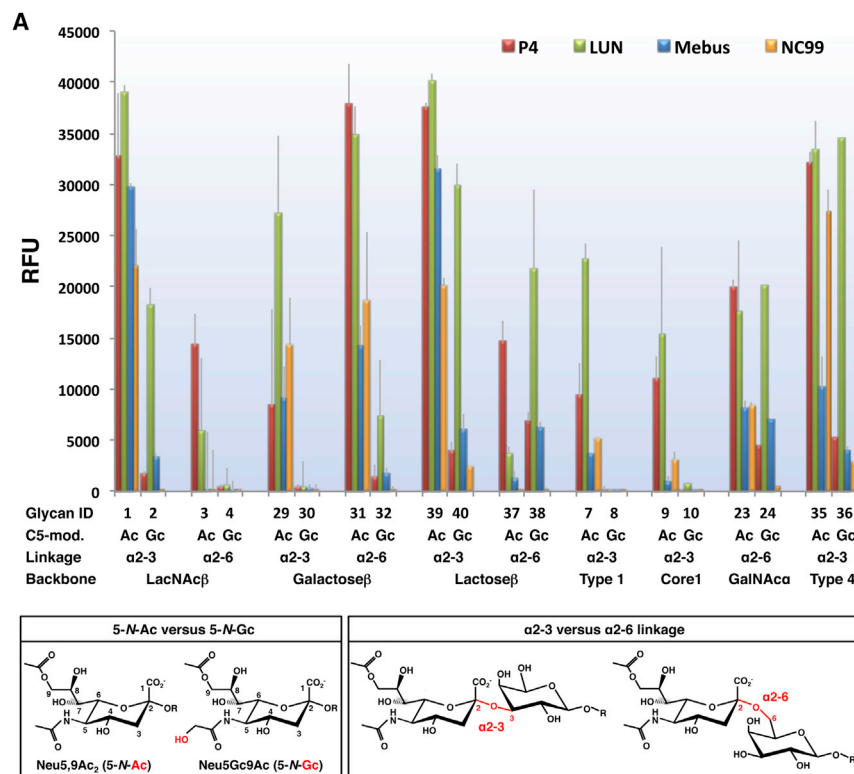
**Figure 3. Glycan Array Analysis**

(A) Differential recognition of 9-*O*-Ac-sialoglycans by the HEs of PToV-P4, BCoV-LUN, BCoV-Mebus, and ECoV-NC99. The library of glycans tested (n = 40; listed in Figure S3) was designed to test the influence on lectin binding of (1) glycosidic linkage of 9-*O*-Ac-Sia (α2-3 versus α2-6) and (2) modifications at Sia atom C5 (*N*-acetylation, 5-*N*-Ac, versus *N*-glycosylation, 5-*N*-Gc; bottom). Data presented as mean ± SD.

(B) HE⁰-Fc virolectins. Summary of ligand preference profiles based on present and published observations (Zeng et al., 2008, Langereis et al., 2009; Langereis et al., 2012). N.A., not analyzed. See also Figure S3.
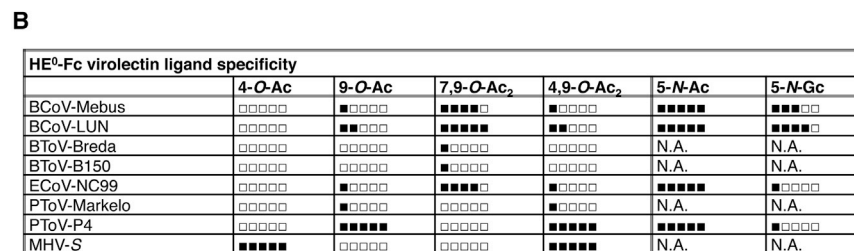
expression patterns did not result from genetic heterogeneity (data not shown). Synthesis of cell-surface P4- and LUN-type 9-*O*-Ac-Sias in HRT-18 cells was sensitive to benzyl *N*-acetyl-α-D-galactosaminide (benzyl-GalNAc) but resistant to *N*-butyl-deoxynojirimycin (NB-DNJ), *N*-butyl-deoxygalactonojirimycin (NB-DGB), and *N*-butyl-deoxymannojirimycin (NB-DMJ), suggesting that they are attached mainly to *O*-linked glycans rather than to *N*-linked sugars or glycolipids (Figure 4B; Gouyer et al., 2001; Platt et al., 1994). As a rule, P4 glycotopes were most abundant and those of NC99 least. Most cells expressing NC99 glycotopes also expressed LUN-type Sias, and in turn, most cells stained by LUN also produced Sias detectable by P4 (Figure 4A). However, relative expression levels of each 9-*O*-Ac-Sia subtype varied widely from one cell to another, and cells that would seem to express LUN- or NC99-type Sias predominantly or even exclusively were also readily detected (Figure 4A). These findings demonstrate that P4, LUN, and NC99 can detect and distinguish between distinct 9-*O*-Ac-Sia populations also in cultured cells.

In two other human cell lines, HeLa and HEK293T, expression of 9-*O*-Ac-Sias appeared more uniform in that virtually all cells produced P4-type Sias and a significant proportion of cells LUN-type Sias as well. These Sias, however, were found exclusively intracellularly (Figures 4C and S4B). Why HeLa and HEK293T cells do not express detectable levels of 9-*O*-Ac-Sias at the plasma membrane is not known. Clearly, an apparent failure of virolectins to bind to the cell surface as determined by L-IFA does not necessarily mean absence of their cognate ligands. Bearing the dynamics of lectin-ligand interactions in mind, in particular the vast incremental effect of ligand valency on apparent lectin affinity (Dam and Brewer, 2010; Dam et al., 2007), the virolectins may predominantly bind to multivalent glycoconjugates with clustered binding sites. Thus, the lack of cell-surface staining in HeLa and HEK293T cells might be explained from a lack of expression of specific cell surface mucin-type
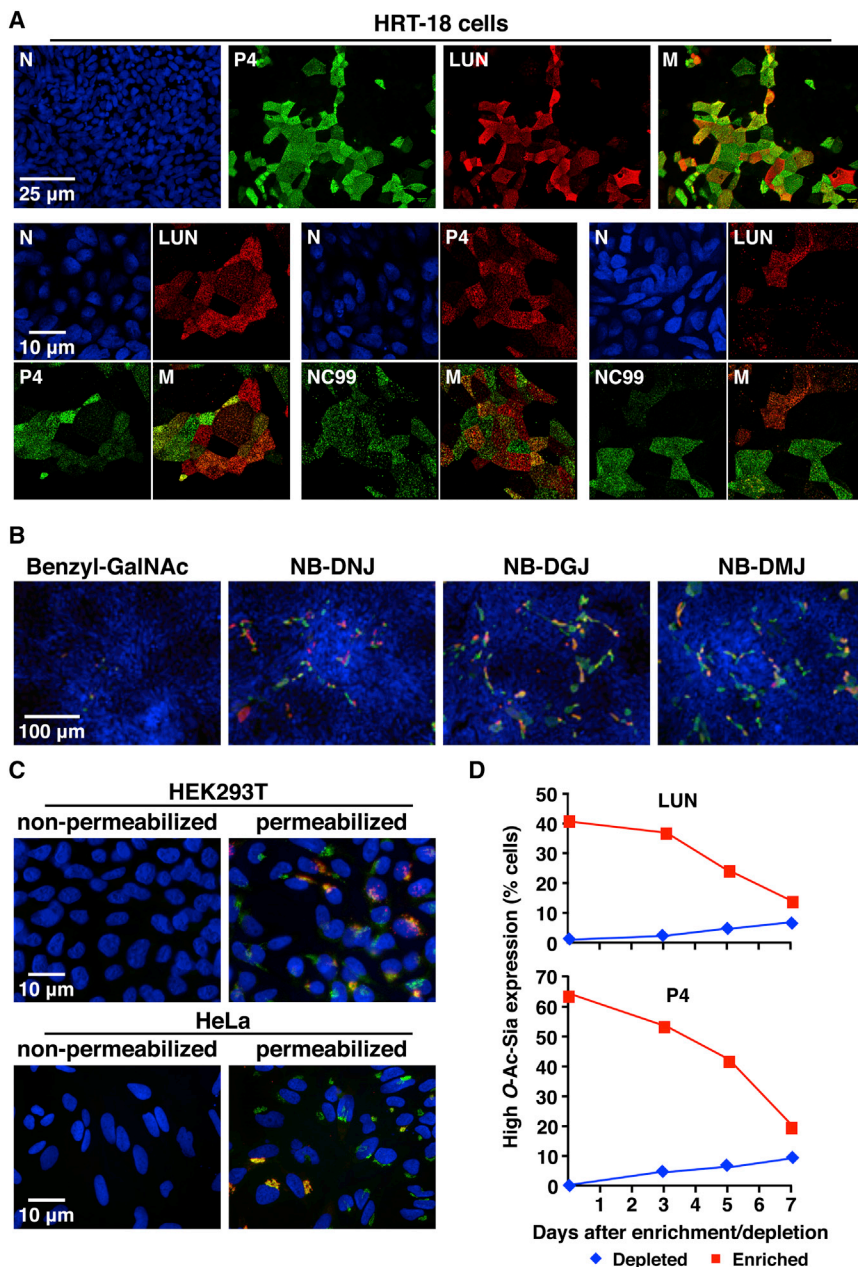
and BCoV-LUN should allow detection in situ of 4-*O*-Ac-Sias, three distinct populations of 9-*O*-Ac-sialoglycans and combinations thereof. For convenience and clarity, we refer to the virolectins and their glycotopes according to virus strain designation (MHV-*S*, P4, LUN, and NC99) in the remainder of the text.

Screening of mammalian continuous cell lines by lectin-immunofluorescence assay (L-IFA) revealed that the Sia populations as detectable by the four virolectins are expressed differentially (Figures 4, 5, and S4). There are considerable differences in expression of Sia subtypes among cell lines and, more remarkably, even among individual cells within the same clonal cell population. All cell lines expressed P4- and LUN-type 9-*O*-Ac-Sias (Table S4), most often in an intracellular compartment reminiscent of the Golgi complex. Indeed, in HeLa cells, 9-*O*-Ac-Sias co-localized with established Golgi markers (Figure S4A).

For a select number of human (HRT-18) and animal cell lines (MDCK and MDBK), extensive surface expression of 9-*O*-Ac-Sias was observed, but, again, only in subpopulations of the cells (1%–10%; Figure 4A). HRT-18 sublineages (n = 3) obtained through single-cell cloning by limiting dilution were indistinguishable from the parental cell line, indicating that the observed Sia

**Figure 4. Differential Expression of *O*-Ac-Sias in Cultured Human Cells as Detected by L-IFA**

(A) Surface expression of P4- (green) and LUN-type (red) Sias in PFA-fixed, non-permeabilized HRT-18 cells. Nuclei (N) stained with Hoechst-33258 (blue). M, merged images.

(B) Sensitivity of cell-surface Sia-*O*-acetylation to glycosylation inhibitors. Cells were stained for P4- and LUN-type Sias after drug treatment (merged images).

(C) Double L-IFA on HEK293T and HeLa cells stained for P4- and LUN-type Sias (merged images).

(D) HRT-18 cells, selected for *O*-Ac-Sia surface expression or lack thereof, revert to Sia heterogeneity. HRT-18 populations, enriched or depleted for cells expressing high levels of P4- or LUN-type Sias by magnetic-activated cell sorting (MACS), were cultured for 3, 5, or 7 days. Cell-surface *O*-Ac-Sia expression was analyzed by flow cytometry.

See also Figure S4 and Table S4.

type 9-*O*-Ac-Sias, albeit again at relative levels that varied from one individual cell to another (Figures 5A and 5B). In contrast to 4-*O*-Ac-Sias, 9-*O*-Ac-Sias were retained intracellularly.

Interestingly, upon treatment of equine cells with *Arthrobacter ureafaciens* siali-dase (*Au*S), most, yet not all, P4-type 9-*O*-Ac-Sias were cleaved (Figure 5A). *Au*S-resistant 9-*O*-Ac-Sias were present invariably in cells that also produced 4-*O*-Ac-Sias. Given that 4-*O*-acetylation protects Sias against cleavage by *Au*S and other sialidases (Corfield et al., 1986), we hypothesized that the *Au*S-resistant Sias detected by P4 were both 9- and 4-*O*-acetylated. Accordingly, in cells treated with *Au*S and sialate-4-*O*-acetylesterase (MHV-*S* HE⁺), all 9-*O*-Ac-Sias were removed (Figure 5A), providing compelling evidence that equine cells produce 4,9-di-*O*- in addition to 4-mono-*O*-Ac-Sias. The results (1) show that nidovirus virolectins can indeed be used to detect and distinguish between different forms of 4-*O*- and 9-*O*-Ac-sialoglycans in individual cells and (2) illustrate how novel types of multiply modified Sias can be discovered and demonstrated in situ, by using viral and microbial SOAEs and sialidases in combination with L-IFA.

### Differential Expression of 4-*O*- and 9-*O*-Ac-Sias in Human and Murine Tissues

Nidovirus HEs also allowed in situ detection of *O*-Ac-Sias in mammalian tissues (Table 1; Figures S5 and S6). In accordance with analytic chemical findings (Rinninger et al., 2006), 4-*O*-Ac-Sias were readily detectable in multiple organs and cell types

glycoproteins that are selectively (and profusely) decorated with *O*-Ac-Sias.

All human cell lines were tested negative by L-IFA for MHV-*S*-type 4-*O*-Ac-Sias (Table S4). This virolectin did bind, however, to cells of mouse and horse, i.e., animal species known to express 4-*O*-Ac-Sias (Aamelfot et al., 2014; Corfield et al., 1976; Rinninger et al., 2006). Whereas in murine LR7 cells, 4-*O*-Ac-Sias were detected exclusively intracellularly (data not shown), in equine cell lines, both intracellular and cell-surface expression were seen (Figures 5 and S4C). Approximately 1% of these cells expressed 4-*O*-Ac-Sias on the surface, whereas in 3%–5%, this Sia was detected only intracellularly (Figure 5A). L-IFA double staining showed that Ederm cells also express LUN- and P4-

## A — Ederm cells

4-O-Ac-Sia | 9-O-Ac-Sia | Merged

mock: MHV-S, P4 / 10 µm
NA: MHV-S, P4
HE⁺ + NA: MHV-S, P4

## B

N | P4 | LUN / 5 µm
Merged | Zoom / 5 µm, 2 µm

## C — FHK cells

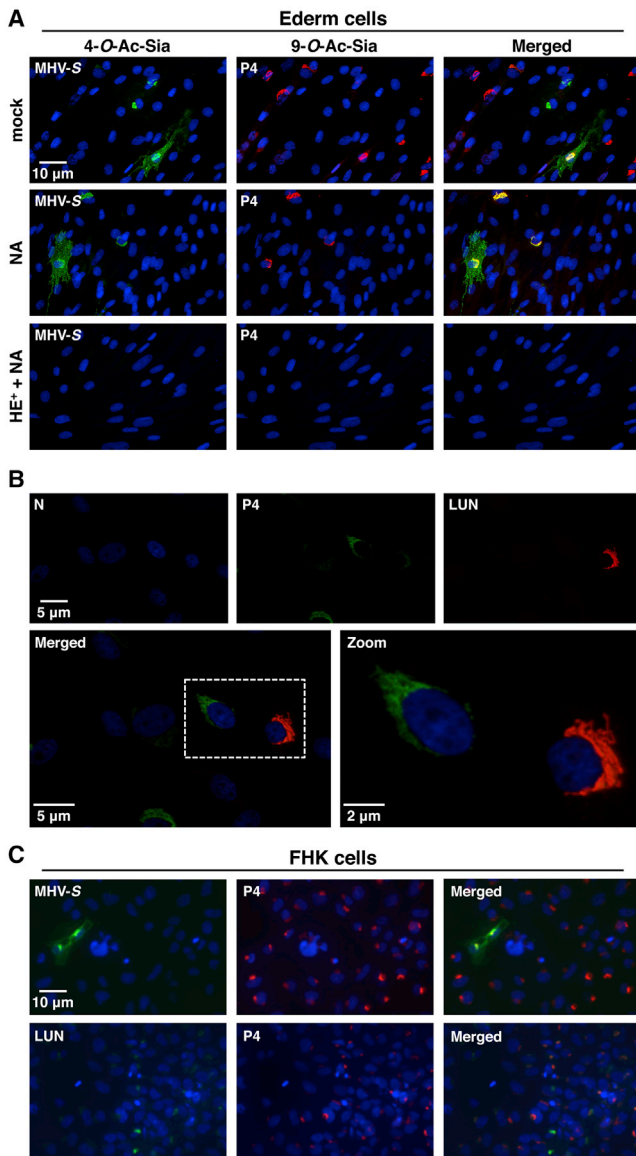MHV-S | P4 | Merged / 10 µm
LUN | P4 | Merged

**Figure 5. Differential Expression of O-Ac-Sias in Equine Cells**
(A) Expression of 4-O- and 9-O-Ac-Sias in Ederm cells as detected by L-IFA with MHV-S (green) and PToV-P4 (red) HE⁰-Fc, respectively. Nuclei were stained with Hoechst-33258 (blue). Permeabilized cells were treated with MHV-S HE⁺-Fc (HE), sialidase (AuS), or both (HE⁺+AuS) or mock treated, prior to L-IFA.
(B) Differential expression of P4- and LUN-type Sias in Ederm cells.
(C) Expression of P4- and LUN-type Sias in FHK cells.
See also Figure S4 and Table S4.

**Table 1. Virolectin Staining Profiles of Human and Murine Tissues**

| | Human Tissue Array | | | Mouse Tissue Array | | |
|---|---|---|---|---|---|---|
| | MHV-S | P4 | LUN | MHV-S | P4 | LUN |
| Adrenal gland | – | + | + | ND | ND | ND |
| Aorta | – | – | – | ND | ND | ND |
| Bladder | – | – | – | – | + | +++ |
| Breast | – | – | – | ND | ND | ND |
| Colon | – | +++ | ++ | ++++ | +++ | ++ |
| Cerebellum | – | + | ++ | – | + | +++ |
| Endothelium | – | – | – | ? | +++ | – |
| Erythrocytes | – | – | – | ? | +++ | +++ |
| Esophagus | – | – | – | – | + | + |
| Eye | ND | ND | ND | – | + | ++ |
| Gray matter | – | + | ++ | – | + | +++ |
| Heart | – | – | – | – | + | + |
| Kidney | – | – | – | – | ++ | ++ |
| Liver | – | – | – | – | + | + |
| Lymph node | – | – | – | ND | ND | ND |
| Lung | – | – | – | – | +++ | +++ |
| Ovary | ND | ND | ND | – | + | + |
| Pancreas | – | + | + | – | ++ | ++ |
| Prostate | – | + | ++ | + | + | ++ |
| Salivary gland | – | ++ | ++ | – | +++ | +++ |
| Skeletal muscle | – | – | – | – | + | + |
| Skin | – | – | – | ++ | + | + |
| Small intestine | – | – | + | – | + | + |
| Spleen | – | – | – | ++ | ++ | ++ |
| Stomach | – | – | – | + | ++ | ++ |
| Thymus | – | – | – | + | + | + |
| Testis | ND | ND | ND | – | – | – |
| Tonsil | – | – | – | ND | ND | ND |
| Thyroid | – | – | – | ND | ND | ND |
| Umbilical cord | – | – | – | ND | ND | ND |
| Uterus | – | – | – | + | ++ | ++ |
| White matter | – | – | – | ND | ND | ND |

ND, not determined. See also Figures S5 and S6.

in mice (most abundantly in the colon; Table 1; Figure S5). All human tissues, however, were negative (Table 1).

9-O-Ac-Sias occur in various tissues in both human and mouse, albeit more profusely and widespread in the latter species (Table 1; Figures S5 and S6). Among noted species differences in Sia expression, murine, but not human, erythrocytes are covered with LUN and P4-type 9-O-Ac-Sias. However, in various organs and cell types, humans and mice display similar 9-O-Ac-Sia profiles, with P4 and LUN glycotopes differentially expressed in comparable fashion. For example, in the prostate, epithelial cells lining the ducts display low-level expression of P4- and high-level expression of LUN-type Sias (Figures S5 and S6). In both species, secreted colonic mucus contains high levels of P4- and LUN-type Sias, but the mucin-producing goblet cells predominantly stain with P4 (Figures S5 and S6). Differential expression of P4 and LUN glycotopes was most conspicuous in the brain, particularly in the cerebellum (Figure 6, S5, and S6). In human and mouse, individual Purkinje cells differed widely in 9-O-Ac-Sia profile, with cells seemingly devoid of 9-O-Ac-Sias, adjacent to ones containing large quantities of P4- and/or LUN-type 9-O-Ac-Sias in granular inclusions in the cell body (Figure 6D). Even within single cells, P4- and
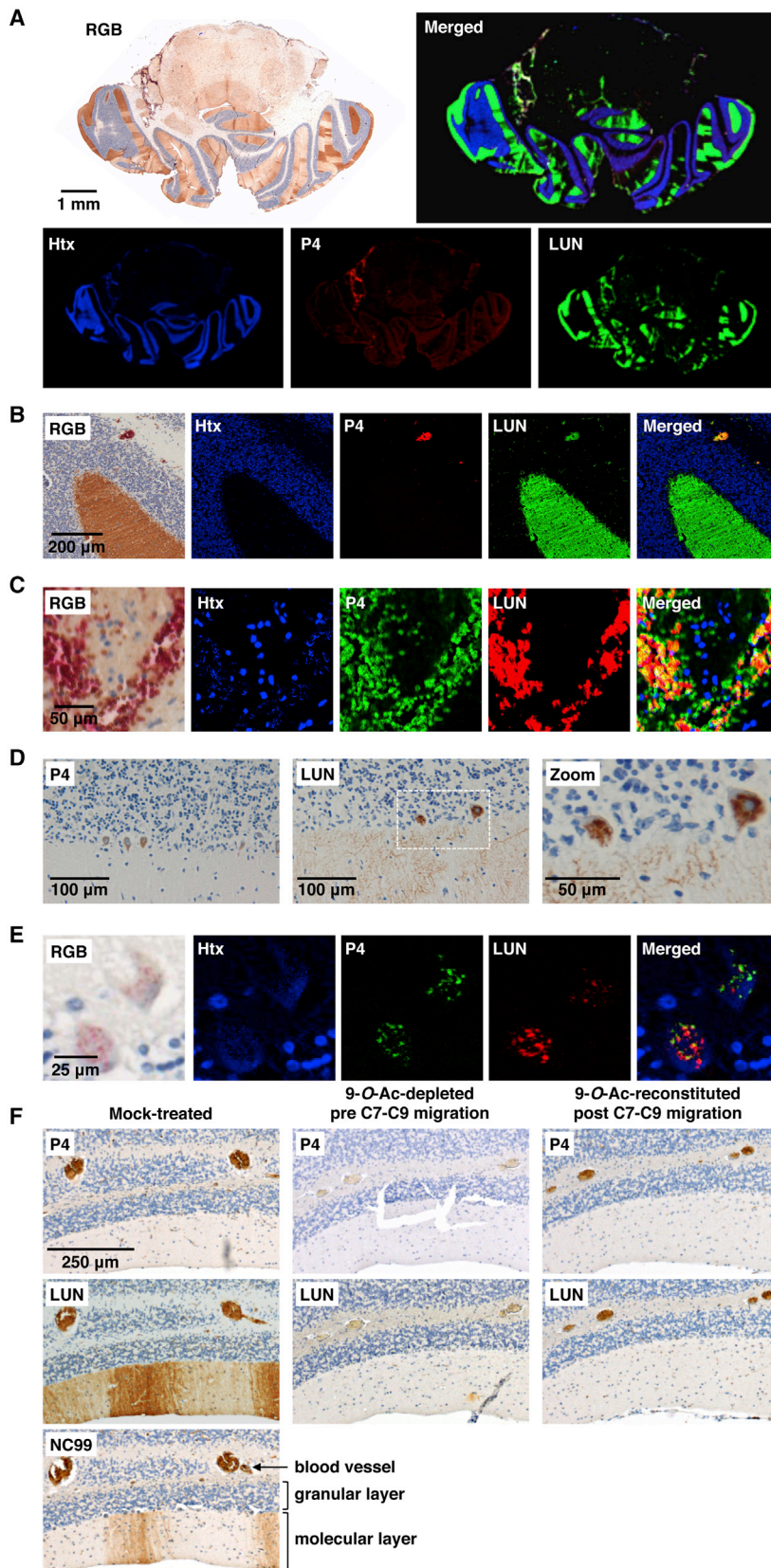
**Figure 6. Differential Expression of P4 and LUN-Type Sias in Human and Murine Cerebellum**

(A) Immunohistochemical staining of cross-sections of mouse brain with P4 (DAB) and LUN (VectorRed). Images in pseudo-colors (hematoxylin [Htx], blue; P4 and LUN in red or green as indicated) were created by spectral analysis.

(B) Blowup of (A).

(C) RBCs in blood vessels stain with P4 and LUN.

(D and E) Differential expression of *O*-Ac-Sias in human Purkinje cells detected by conventional light microscopy (D) or by double lectin staining and spectral analysis (E) as in (A).

(F) Serial sections of mouse cerebellum stained with virolectins after mock treatment (left), enzymatic depletion of 9-*O*-Ac-Sia moieties (middle), or subsequent C7-to-C9 *O*-acetyl migration (right).

LUN-type 9-O-Ac-Sias were often found in different compartments (Figure 6E). Most strikingly, in the mouse, the dendritic arbors of 9-O-Sia-producing Purkinje neurons stained for LUN-type 9-O-Ac-Sias only, creating a striated, bar code-like pattern in the molecular layer in the cerebellar cortex (Figures 6A–6C, 6F, and S5; note the robust staining of RBCs by P4). This pattern was less conspicuous in the human cerebellum, but also here, dendritic arbors stained with LUN and not with P4 (Figure S6). NC99- and LUN-staining of Purkinje cells resulted in identical patterns in serial sections of mouse cerebellum (Figure 6F), arguing against the lack of P4-binding resulting from exclusive expression of 5-N-Gc-Sias (Figure 3). In fact, Neu5Gc is exceedingly rare even in the murine brain (Davies and Varki, 2013) and completely absent in humans (Chou et al., 1998). To test whether lack of P4 binding was due to prevalent Sia-7,9-di-O-acetylation in Purkinje cells, sections of mouse cerebellum were enzymatically depleted for 9-O-Ac-Sias while preserving 7-O-Ac-Sias. In consequence, staining of Purkinje cells and RBCs by both P4 and LUN was lost. Subsequent pH/temperature-induced C7-to-C9 migration of the remaining Sia-7-O-Ac moieties restored staining of RBCs by P4, but saliently, that by LUN as well. While these findings provide independent confirmation that erythrocytes do express 7,9-di-O-Ac-Sias (presenting a source for 9-mono-O-Ac-Sias upon experimentally induced C7-to-9-O-Ac migration), they also show that in tissue sections, under the conditions applied, LUN binds 9-mono-O-Ac-Sias too (Figure 6F). Importantly, the conditions that restored Sia 9-O-acetylation on RBCs did not generate P4 glycotopes in Purkinje cell dendrites, nor salvaged LUN binding. It would thus appear that the Sias in the mouse cerebellum are mainly 9-mono-O-acetylated and that the differential staining of Purkinje cells by P4 and LUN must be ascribed to a particular glycan structure and/or to Sia modifications, additional to 9-O-acetylation, that are tolerated by LUN, but not by P4. Although the LUN glycotopes in the cerebellum await definitive identification, our findings do underscore the diversity and complexity of naturally occurring O-Ac-sialoglycans and their cell(-type)-specific differential expression. It is fair to assume that like the virolectins used here, cellular lectins distinguish between these Sia populations and that regulation of lectin binding, through controlled Sia-O-acetylation/de-O-acetylation, may have far-reaching biological effects and consequences.

### Viral Preference for O-Ac-Sialoglycan Receptor Determinants and Host Tropism

Many viruses encode proteins that recognize, bind to, and modify Sia-glycotopes with exquisite specificity (Matrosovich et al., 2013; Neu et al., 2011; Stehle and Khan, 2014). Here, we demonstrate that nidoviruses are even more fastidious with respect to Sia receptor usage than appreciated so far. For all nidovirus HEs studied, the ligand specificity and SOAE substrate preference are in close accord (Figures 3B and S2C), indicative of co-evolution of lectin and esterase domains. Apparently, Sia subtype preference correlates with viral host tropism. The HE proteins of PToV-Markelo and -P4 are highly divergent, with only 77% identity in their ectodomains, yet both display a preference for 9-mono-O-Ac-Sias. In contrast, the HEs of BCoV and those of two distinct BToV lineages (represented by strains

Breda and B150), all preferentially bind to 7,9-di-O-acetylated ligands instead (Figure 3B). It would seem that in toroviruses and lineage A betacoronaviruses, HE selectivity for O-Ac-Sia receptor subtypes arose as an adaptation to the "sialomes" of the target tissues in their respective hosts and that the shared preference of bovine corona- and toroviruses for 7,9-di-O-Ac-Sias resulted from convergent evolution.

### Cell-to-Cell Variability in O-Ac-Sialoglycan Synthesis: Stochastic Gene Expression or Determinism?

Our results not only advance the understanding of virus-Sia interactions and virus evolution but also, more importantly, show how virolectins can be exploited as tools in sialoglycomics and explorative glycobiology. One of our most striking observations is the phenotypic heterogeneity among individual cells of homogenous clonal cell lines. Cells differed not only in the extent to which they expressed O-Ac-Sias but also in the types of O-Ac-Sias produced. Apparently, even in populations of tissue culture cells, cell-to-cell variation occurs in the expression of enzymes required for the biosynthesis or degradation of O-Ac-Sias and/or of the glycoconjugates that are carry these sugars. This cell-to-cell variability may be attributed to stochasticity ("noisy" gene expression) but perhaps more likely arises from deterministic spatiotemporal influences such as population context and/or cellular crowding (Snijder and Pelkmans, 2011). Indeed, O-Ac-Sia-expressing cells tend to occur in islets (Figure 4A). HRT-18 subpopulations, selected by lectin-MACS for O-Ac-Sia surface expression or lack thereof, reverted to Sia heterogeneity over time (~7 days) and a limited number of cell generations (Figure 4D), reminiscent of the short-term phenotypic memory seen in other examples of cell-to-cell variability (Mariani et al., 2010; Sigal et al., 2006). Our findings raise questions regarding the triggers that induce or prevent Sia-O-acetylation in individual cells but also offer ways and means to study this phenomenon and the mechanisms involved. On a more technical note, our observations illustrate the intricacies of (sialo)glycobiology and underline the pitfalls and limitations of functional glycomics approaches based upon averaging sialoglycan content of cell populations and whole tissue samples.

### O-Ac-Sialoglycan Expression in Mammals: Cell, Tissue, and Species Specificity

Comparative analysis of mouse and human revealed important differences in Sia repertoire and sialylation profiles. For example, 4-O-Ac-Sias, abundant in mice (and horses), were not detected by virolectin histochemistry in humans, either in cultured cells or in tissues. Of two reports of 4-O-Ac Sias in humans, one involved a Sia variant, Neu4Ac5Gc (Miyoshi et al., 1986), of established non-human, dietary origin (Banda et al., 2012; Tangvoranuntakul et al., 2003). The other observation of Neu4,5Ac$_2$ and 9-O-lactylated Neu4,5Ac$_2$ in human erythrocytes (Bulai et al., 2003) as yet awaits independent confirmation. We cannot exclude that 4-O-Ac-Sias are expressed infrequently, in concentrations below our detection levels, and/or specifically in distinct types of tissues and cells absent from our human tissue arrays. Yet, the data lead us to consider that humans might not produce this type of Sia after all. Such a deficiency would not be without precedent: defective

synthesis of Neu5Gc sets us apart even from our closest non-human relatives (Chou et al., 2002).

9-*O*-Ac-sialoglycans occur in both human and mouse and apparently are expressed in a well-coordinated cell- and tissue-specific fashion. There are species differences in tissue distribution of distinct 9-*O*-Ac-Sias, and, in general, these sugars are more widely and abundantly present in the mouse. More importantly, however, in several key organs and tissues, particularly in the brain, mice and humans share highly similar 9-*O*-Ac-Sia expression profiles, suggestive of evolutionary and functional conservation.

## Conclusions and Perspectives

The present work opens avenues for the exploration of the vast and uncharted territory that is sialoglycobiology. The challenge ahead will be to answer the many questions raised by present observations. For example, how is *O*-acetylation of Sias regulated at the level of individual cells? What are the cues to activate or inactivate the cellular SOATs and SOAEs to establish, maintain, and alter a particular cell (surface) sialylation profile? Which enzymes and signaling pathways are involved? Which glycoconjugates are decorated with *O*-Ac-Sias? How does Sia-*O*-acetylation and the regulation thereof relate to cell function? Are there, for example, functional differences between Purkinje cell populations that express *O*-Ac-Sias and those that do not, and why is there a preference for expression of LUN- rather than P4-type Sias in these neurons? The resources and methodology described here will help to settle these outstanding issues. Moreover, our understanding of the molecular basis of ligand and substrate recognition by nidovirus HEs may allow the construction of designer lectins and enzymes of even higher affinity and more narrow specificity to further facilitate such studies.

## EXPERIMENTAL PROCEDURES

### Protein Expression and Purification

Nidovirus HE ectodomains and influenza virus C HEF-1 were transiently expressed in HEK293T cells as fusion proteins with a C-terminal Fc domain of human IgG1 or that of mouse or bovine IgG2a as described previously (Zeng et al., 2008). HE-Fc proteins, purified from cell supernatants by protein A-affinity chromatography, were eluted with 0.1 M citric acid (pH 3.0). Eluates were neutralized with 1 M Tris buffer (pH 8.8) (0.2 M final concentration) and dialyzed for 16 hr at 4°C against PBS.

### Hemagglutination Assay

Hemagglutination assays were performed with rat RBCs (*Rattus norvegicus* strain Wistar; 50% suspension in PBS) and 2-fold serial dilutions of HE[0]-Fc proteins (starting at 0.1 μg/μl) as described previously (Zeng et al., 2008). For specific depletion of cell-surface *O*-Ac-Sias, RBCs were (mock) treated with BCoV-Mebus, MHV-*S*, PToV-Markelo, or BToV-Breda HE[+]-Fc (0.2 μg/μl) for 2 hr at 37°C, washed with PBS, and resuspended to 50%. Animal use was in accordance with legislation of the Netherlands and the European Union and approved by the ethics committee for animal experiments of Utrecht University.

### Solid-Phase Lectin Binding Assay

Maxisorp 96-well plates (Nunc) were coated for 16 hr at 4°C with native BSM (10 μg/ml in PBS [pH 6.5]; 100 μl/well) or with BSM preparations, depleted for specific *O*-Ac-Sias. For the production of BSM preparations with defined *O*-Ac-Sia content, see the Supplemental Experimental Procedures. Two-fold serial dilutions of HE[0]-Fc lectins in blocking buffer (PBS, 0.05% Tween-20,

2% BSA) were applied (starting at 0.1 μg/μl, 100 μl/well) for 1 hr at 37°C. Incubation was then continued with horseradish peroxidase (HRP)-conjugated goat-α-human immunoglobulin (IgG) antibody (Southern Biotech; 1:1,000 in blocking buffer) for 30 min at 37°C. Washing was with PBS, 0.05% Tween-20. Bound HE[0]-Fc was detected with TMB Super Slow One Component HRP Microwell Substrate (BioFX). Optical densities (ODs) were measured at 450 nm.

For on-the-plate depletion of *O*-Ac-Sia receptors, native BSM coated on Maxisorp plates was (mock) treated with 2-fold serial dilutions of BCoV-Mebus, PToV-P4 (starting at 0.1 ng/μl), or BToV-Breda (starting at 5 ng/μl) HE[+] enzymes in PBS (pH 6.5) for 2 hr at 37°C (100 μl/well). sp-LBA with BCoV-Mebus (5 ng/μl) and PToV-P4 (1 ng/μl) lectins were as described. Depletion of *O*-Ac-Sia receptors was calculated from the inverse of lectin binding measurements, expressed in percentages.

### Lectin-Immunofluorescence Assay of Cultured Cells

Cell monolayers on glass coverslips were fixed with PFA (3.7% in PBS, 15 min), either left non-permeabilized or permeabilized with PBS, 0.1% Triton X-100 (10 min), successively incubated (1 hr each) with blocking buffer (PBS, 0.05% Tween-20, 2% BSA) and with HE[0]-Fc lectins (MHV-*S*, 50 μg/ml; PToV-P4, 20 μg/ml; ECoV-NC99, 100 μg/ml; BCoV-LUN, 100 μg/ml; concentrations used were 2- to 4-fold above saturation as determined by LBA with 2-fold serial dilutions of each lectin), and then for 30 min with goat-α-human IgG-Dylight488 and/or goat-α-bovine IgG-Dylight549 (Jackson ImmunoResearch; 1:100), and with Hoechst-33258 (1:200). All incubations were in blocking buffer. Washing was performed with PBS, 0.05% Tween-20. The cells, embedded in FluorSave (Calbiochem), were examined by standard fluorescence microscopy (Leica DMRE).

Inhibitors were added to culture supernatants of HRT-18 cells (Benzyl-Gal-NAc, 2.5 mM; NB-DNJ, 0.2 mM; NB-DGB, 0.1 mM; NB-DMJ, 0.1 mM). Incubation was continued for 72 hr. Cells were fixed and stained with PToV-P4 and BCoV-LUN HE[0]-Fc lectins as described above. To de-*O*-acetylate or remove cell-surface Sias prior to L-IFA, PFA-fixed Ederm cells were incubated for 2 hr at 37°C with PBS, containing 20 μg/ml MHV-*S* HE[+]-Fc or 100 mU/ml *Arthrobacter ureafaciens* sialidase (AuS; Sigma-Aldrich), respectively.

### Lectin Staining of Mammalian Tissues

Paraffin-embedded tissue sections (Gentaur; mouse tissue array, AMS541; mouse brain, T2334035; human tissue array, AC1; human cerebellum, T2234039) were dewaxed in xylene and rehydrated. Endogenous peroxidases were inactivated with peroxide (0.3% in methanol). For indirect chromogenic detection of *O*-Ac-Sias, tissue sections were successively incubated with HE[0]-Fc virolectins (20 or 40 μg/ml; optimal concentrations determined as described for L-IFA), with biotinylated goat-α-human IgG or goat-α-mouse IgG antibodies (Sigma-Aldrich; 1:250; lectins and antibodies all diluted in blocking buffer), with avidin-biotin HRPO complex (ABC-PO staining kit, Thermo Scientific), and with 3,3′-diaminobenzidine (DAB; Sigma-Aldrich). Blocking, incubations, and washing was as for L-IFA. Tissue sections were counterstained with Mayer's hematoxylin, embedded in Eukitt mounting medium (Fluka) and examined by standard light microscopy. Simultaneous detection of P4- and LUN-type Sias in human cells was performed with PToV-P4 (20 μg/ml) and BCoV-LUN (40 μg/ml) HE[0] fused to mouse and bovine Fc-domains, respectively, and with a combination of HRP-conjugated goat-α-mouse IgG- and alkaline phosphatase (AP)-conjugated goat-α-bovine IgG antibodies (Jackson ImmunoResearch). Tissue sections were stained for AP with the VectorRed AP Substrate kit (Vector) and for HRPO with DAB, and further processed as above. Mouse tissues were treated likewise, but with HE[0]s fused to human or bovine IgG Fc-domains. Spectral analysis (460 to 660 nm at 10-nm intervals) was performed as described (van der Loos, 2008) using a Leica BM5000 microscope (Leica Microsystems) with a Nuance VIS-FL Multispectral Imaging System (Cambridge Research Instrumentation). Images were analyzed with Nuance 2.4.

### Glycan Sialoglycan Microarray

Glycan microarrays were prepared with epoxide-derivatized slides and processed, essentially as described (Padler-Karavani et al., 2012). For detailed procedures, see the Supplemental Experimental Procedures.

## Molecular Docking

The structure of α-Neu5,7,9Ac$_3$2Me was drawn using Chemsketch (Advanced Chemistry Development). Docking simulations between BCoV-Mebus HE (PDB: 3CL5) and α-Neu5,7,9Ac$_3$2Me were performed using AutoDock Vina software (Scripps Research Institute) at a box size of 20 × 15 × 15 Å, with HE set as a rigid unit and with the ligand allowed to be flexible and adaptable. Docking of α-Neu5,9Ac$_2$2Me predicted a Sia topology identical to that seen in the crystal structure of the HE/α-Neu4,5,9Ac$_3$2Me complex thus validating the simulation conditions (data not shown).

## SUPPLEMENTAL INFORMATION

Supplemental Information includes Supplemental Experimental Procedures, six figures, and four tables and can be found with this article online at http://dx.doi.org/10.1016/j.celrep.2015.05.044.

## AUTHOR CONTRIBUTIONS

## ACKNOWLEDGMENTS

## REFERENCES

Aamelfot, M., Dale, O.B., Weli, S.C., Koppang, E.O., and Falk, K. (2014). The in situ distribution of glycoprotein-bound 4-O-Acetylated sialic acids in vertebrates. Glycoconj. J. 31, 327–335.

Banda, K., Gregg, C.J., Chow, R., Varki, N.M., and Varki, A. (2012). Metabolism of vertebrate amino sugars with N-glycolyl groups: mechanisms underlying gastrointestinal incorporation of the non-human sialic acid xeno-autoantigen N-glycolylneuraminic acid. J. Biol. Chem. 287, 28852–28864.

Bulai, T., Bratosin, D., Pons, A., Montreuil, J., and Zanetta, J.P. (2003). Diversity of the human erythrocyte membrane sialic acids in relation with blood groups. FEBS Lett. 534, 185–189.

Büll, C., Stoel, M.A., den Brok, M.H., and Adema, G.J. (2014). Sialic acids sweeten a tumor's life. Cancer Res. 74, 3199–3204.

Cariappa, A., Takematsu, H., Liu, H., Diaz, S., Haider, K., Boboila, C., Kalloo, G., Connole, M., Shi, H.N., Varki, N., et al. (2009). B cell antigen receptor signal strength and peripheral B cell development are regulated by a 9-O-acetyl sialic acid esterase. J. Exp. Med. 206, 125–138.

Chou, H.H., Takematsu, H., Diaz, S., Iber, J., Nickerson, E., Wright, K.L., Muchmore, E.A., Nelson, D.L., Warren, S.T., and Varki, A. (1998). A mutation in human CMP-sialic acid hydroxylase occurred after the Homo-Pan divergence. Proc. Natl. Acad. Sci. USA 95, 11751–11756.

Chou, H.H., Hayakawa, T., Diaz, S., Krings, M., Indriati, E., Leakey, M., Paabo, S., Satta, Y., Takahata, N., and Varki, A. (2002). Inactivation of CMP-N-acetyl-neuraminic acid hydroxylase occurred prior to brain expansion during human evolution. Proc. Natl. Acad. Sci. USA 99, 11736–11741.

Corfield, A.P., Ferreira do Amaral, C., Wember, M., and Schauer, R. (1976). The metabolism of O-acyl-N-acylneuraminic acids. Biosynthesis of O-acylated sialic acids in bovine and equine submandibular glands. Eur. J. Biochem. 68, 597–610.

Corfield, A.P., Sander-Wewer, M., Veh, R.W., Wember, M., and Schauer, R. (1986). The action of sialidases on substrates containing O-acetylsialic acids. Biol. Chem. Hoppe Seyler 367, 433–439.

Crocker, P.R., Paulson, J.C., and Varki, A. (2007). Siglecs and their roles in the immune system. Nat. Rev. Immunol. 7, 255–266.

Dam, T.K., and Brewer, C.F. (2010). Multivalent lectin-carbohydrate interactions energetics and mechanisms of binding. Adv. Carbohydr. Chem. Biochem. 63, 139–164.

Dam, T.K., Gerken, T.A., Cavada, B.S., Nascimento, K.S., Moura, T.R., and Brewer, C.F. (2007). Binding studies of α-GalNAc-specific lectins to the α-GalNAc (Tn-antigen) form of porcine submaxillary mucin and its smaller fragments. J. Biol. Chem. 282, 28256–28263.

Davies, L.R., and Varki, A. (2013). Why Is N-glycolylneuraminic acid rare in the vertebrate brain? Top. Curr. Chem.

de Groot, R.J. (2006). Structure, function and evolution of the hemagglutinin-esterase proteins of corona- and toroviruses. Glycoconj. J. 23, 59–72.

Deng, L., Chen, X., and Varki, A. (2013). Exploration of sialic acid diversity and biology using sialoglycan microarrays. Biopolymers 99, 650–665.

Ghosh, S., Bandyopadhyay, S., Mukherjee, K., Mallick, A., Pal, S., Mandal, C., Bhattacharya, D.K., and Mandal, C. (2007). O-acetylation of sialic acids is required for the survival of lymphoblasts in childhood acute lymphoblastic leukemia (ALL). Glycoconj. J. 24, 17–24.

Gouyer, V., Leteurtre, E., Zanetta, J.P., Lesuffleur, T., Delannoy, P., and Huet, G. (2001). Inhibition of the glycosylation and alteration in the intracellular trafficking of mucins and other glycoproteins by GalNAcalpha-O-bn in mucosal cell lines: an effect mediated through the intracellular synthesis of complex GalNAcalpha-O-bn oligosaccharides. Front. Biosci. 6, D1235–D1244.

Irie, A., Koyama, S., Kozutsumi, Y., Kawasaki, T., and Suzuki, A. (1998). The molecular basis for the absence of N-glycolylneuraminic acid in humans. J. Biol. Chem. 273, 15866–15871.

Kamerling, J.P., and Gerwig, G.J. (2006). Structural analysis of naturally occurring sialic acids. Methods Mol. Biol. 347, 69–91.

Kamerling, J.P., Schauer, R., Shukla, A.K., Stoll, S., Van Halbeek, H., and Vliegenthart, J.F.G. (1987). Migration of O-acetyl groups in N,O-acetylneuraminic acids. Eur. J. Biochem. 162, 601–607.

Klein, A., and Roussel, P. (1998). O-acetylation of sialic acids. Biochimie 80, 49–57.

Klein, A., Krishna, M., Varki, N.M., and Varki, A. (1994). 9-O-acetylated sialic acids have widespread but selective expression: analysis using a chimeric dual-function probe derived from influenza C hemagglutinin-esterase. Proc. Natl. Acad. Sci. USA 91, 7782–7786.

Kozak, R.P., Royle, L., Gardner, R.A., Fernandes, D.L., and Wuhrer, M. (2012). Suppression of peeling during the release of O-glycans by hydrazinolysis. Anal. Biochem. 423, 119–128.

Krishna, M., and Varki, A. (1997). 9-O-Acetylation of sialomucins: a novel marker of murine CD4 T cells that is regulated during maturation and activation. J. Exp. Med. 185, 1997–2013.

Langereis, M.A., Zeng, Q., Gerwig, G.J., Frey, B., von Itzstein, M., Kamerling, J.P., de Groot, R.J., and Huizinga, E.G. (2009). Structural basis for ligand and substrate recognition by torovirus hemagglutinin esterases. Proc. Natl. Acad. Sci. USA 106, 15897–15902.

Langereis, M.A., Zeng, Q., Heesters, B.A., Huizinga, E.G., and de Groot, R.J. (2012). The murine coronavirus hemagglutinin-esterase receptor-binding site: a major shift in ligand specificity through modest changes in architecture. PLoS Pathog. 8, e1002492.

Mariani, L., Schulz, E.G., Lexberg, M.H., Helmstetter, C., Radbruch, A., Löhning, M., and Höfer, T. (2010). Short-term memory in gene induction reveals the regulatory principle behind stochastic IL-4 expression. Mol. Syst. Biol. *6*, 359.

Matrosovich, M., Herrler, G., and Klenk, H.D. (2013). Sialic acid receptors of viruses. Top. Curr. Chem.

Miyoshi, I., Higashi, H., Hirabayashi, Y., Kato, S., and Naiki, M. (1986). Detection of 4-*O*-acetyl-*N*-glycolylneuraminyl lactosylceramide as one of tumor-associated antigens in human colon cancer tissues by specific antibody. Mol. Immunol. *23*, 631–638.

Mukherjee, K., Chava, A.K., Mandal, C., Dey, S.N., Kniep, B., Chandra, S., and Mandal, C. (2008). *O*-acetylation of GD3 prevents its apoptotic effect and promotes survival of lymphoblasts in childhood acute lymphoblastic leukaemia. J. Cell. Biochem. *105*, 724–734.

Neu, U., Bauer, J., and Stehle, T. (2011). Viruses and sialic acids: rules of engagement. Curr. Opin. Struct. Biol. *21*, 610–618.

Padler-Karavani, V., Hurtado-Ziola, N., Pu, M., Yu, H., Huang, S., Muthana, S., Chokhawala, H.A., Cao, H., Secrest, P., Friedmann-Morvinski, D., et al. (2011). Human xeno-autoantibodies against a non-human sialic acid serve as novel serum biomarkers and immunotherapeutics in cancer. Cancer Res. *71*, 3352–3363.

Padler-Karavani, V., Song, X., Yu, H., Hurtado-Ziola, N., Huang, S., Muthana, S., Chokhawala, H.A., Cheng, J., Verhagen, A., Langereis, M.A., et al. (2012). Cross-comparison of protein recognition of sialic acid diversity on two novel sialoglycan microarrays. J. Biol. Chem. *287*, 22593–22608.

Parameswaran, R., Lim, M., Arutyunyan, A., Abdel-Azim, H., Hurtz, C., Lau, K., Müschen, M., Yu, R.K., von Itzstein, M., Heisterkamp, N., and Groffen, J. (2013). *O*-acetylated *N*-acetylneuraminic acid as a novel target for therapy in human pre-B acute lymphoblastic leukemia. J. Exp. Med. *210*, 805–819.

Pillai, S. (2013). Rethinking mechanisms of autoimmune pathogenesis. J. Autoimmun. *45*, 97–103.

Platt, F.M., Neises, G.R., Karlsson, G.B., Dwek, R.A., and Butters, T.D. (1994). *N*-butyldeoxygalactonojirimycin inhibits glycolipid biosynthesis but does not affect *N*-linked oligosaccharide processing. J. Biol. Chem. *269*, 27108–27114.

Rinninger, A., Richet, C., Pons, A., Kohla, G., Schauer, R., Bauer, H.C., Zanetta, J.P., and Vlasak, R. (2006). Localisation and distribution of *O*-acetylated *N*-acetylneuraminic acids, the endogenous substrates of the hemagglutinin-esterases of murine coronaviruses, in mouse tissue. Glycoconj. J. *23*, 73–84.

Schauer, R. (2009). Sialic acids as regulators of molecular and cellular interactions. Curr. Opin. Struct. Biol. *19*, 507–514.

Shi, W.X., Chammas, R., and Varki, A. (1996). Regulation of sialic acid 9-*O*-acetylation during the growth and differentiation of murine erythroleukemia cells. J. Biol. Chem. *271*, 31517–31525.

Shi, W.X., Chammas, R., and Varki, A. (1998). Induction of sialic acid 9-*O*-acetylation by diverse gene products: implications for the expression cloning of sialic acid *O*-acetyltransferases. Glycobiology *8*, 199–205.

Sigal, A., Milo, R., Cohen, A., Geva-Zatorsky, N., Klein, Y., Liron, Y., Rosenfeld, N., Danon, T., Perzov, N., and Alon, U. (2006). Variability and memory of protein levels in human cells. Nature *444*, 643–646.

Sjoberg, E.R., Powell, L.D., Klein, A., and Varki, A. (1994). Natural ligands of the B cell adhesion molecule CD22 beta can be masked by 9-O-acetylation of sialic acids. J. Cell Biol. *126*, 549–562.

Smits, S.L., Gerwig, G.J., van Vliet, A.L.W., Lissenberg, A., Briza, P., Kamerling, J.P., Vlasak, R., and de Groot, R.J. (2005). Nidovirus sialate-*O*-acetylesterases: evolution and substrate specificity of coronaviral and toroviral receptor-destroying enzymes. J. Biol. Chem. *280*, 6933–6941.

Snijder, B., and Pelkmans, L. (2011). Origins of regulated cell-to-cell variability. Nat. Rev. Mol. Cell Biol. *12*, 119–125.

Stehle, T., and Khan, Z.M. (2014). Rules and exceptions: sialic acid variants and their role in determining viral tropism. J. Virol. *88*, 7696–7699.

Surolia, I., Pirnie, S.P., Chellappa, V., Taylor, K.N., Cariappa, A., Moya, J., Liu, H., Bell, D.W., Driscoll, D.R., Diederichs, S., et al. (2010). Functionally defective germline variants of sialic acid acetylesterase in autoimmunity. Nature *466*, 243–247.

Tangvoranuntakul, P., Gagneux, P., Diaz, S., Bardor, M., Varki, N., Varki, A., and Muchmore, E. (2003). Human uptake and incorporation of an immunogenic nonhuman dietary sialic acid. Proc. Natl. Acad. Sci. USA *100*, 12045–12050.

Trott, O., and Olson, A.J. (2010). AutoDock Vina: improving the speed and accuracy of docking with a new scoring function, efficient optimization, and multithreading. J. Comput. Chem. *31*, 455–461.

van der Loos, C.M. (2008). Multiple immunoenzyme staining: methods and visualizations for the observation with spectral imaging. J. Histochem. Cytochem. *56*, 313–328.

Zeng, Q., Langereis, M.A., van Vliet, A.L.W., Huizinga, E.G., and de Groot, R.J. (2008). Structure of coronavirus hemagglutinin-esterase offers insight into corona and influenza virus evolution. Proc. Natl. Acad. Sci. USA *105*, 9065–9069.